

The Dynamic Characteristics of Hydraulic-Mechanical Constant Speed Drive

Y Vul¹, R Kalyakin^{1,2} and A Shablovskiy¹

¹Bauman Moscow State Technical University

²E-mail: defendly@gmail.com

Annotation: This paper discusses the development of a mathematical model for the constant speed drive, comprising the power supply of an aircraft power grid. The model is developed in the form of equations of dynamics of the drive main components, such as differential, volumetric hydraulic transmission, centrifugal regulator, auxiliary pumps, as well as using the AMESim calculation package. The model has been verified using experimental data of the AC frequency responses of the existing unit to various influences. The models obtained allow to conclude about the stability of the system, and to optimize the control system parameters.

Introduction

Three-phase AC voltage with frequency of 400 Hz is required to power on-board electrical system of most aircrafts. The most commonly used power supply of this type of electricity is a bunch of alternator and a constant speed drive called ‘integrated generator drive’ (GD). Due to the fact that aircraft developers need to increase the power of the power source and strict requirements to its weight and size properties [1], the best solutions in the design of the unit are required. To select the optimal parameters of the unit and calculate its stability, its mathematical model is necessary. Mathematical modeling of hydraulic-mechanical devices is an important problem [2]–[6].

Research on the choice of an optimal power source for the power supply systems of aircraft is still underway. Papers [7] conclude that there is no single solution for the choice of aircraft power generation systems. For each individual case, a structural and functional method of analysis and synthesis of electric power systems is required.

The study of the constant speed drive operation in the range of zero revolutions of a hydraulic transmission is demonstrated in the paper [8]. In the paper [9], generator model is used to detect and prevent its faults during the flight.

The GD control system ensures the frequency constancy of current with a deviation from the rated value of no more than $\pm 2\%$ at a change of loading in the grid, ambient temperature, or rotation velocity of the aircraft engine to which the input shaft of GD is connected via an aircraft accessory box.

The GD principle of operation is as follows. Mechanical energy at the input is divided into two streams, one of which goes through a mechanical transmission with a constant transfer coefficient, while the other goes through a hydrostatic drive with a variable transfer coefficient. Then, both streams are summed up using a differential gear, which results in the maintenance of a constant rotation frequency of a generator shaft within the tolerance regardless of the engine shaft speed, load in the grid, or ambient temperature. Control of the hydrostatic drive is performed by a centrifugal



regulator and an associated servo piston that moves the inclined washer of the adjustable hydraulic machine. For more details about the operation of the constant speed drive, refer to paper [10].

Method

We will study the dynamic characteristics of GD using its mathematical model. This requires to compile the dynamics equations for the main assemblies of the unit and utilize AMESim application package which allows to perform one-dimensional multi-physical modeling [11–13]. The main assemblies of the unit include a generator, differential gear, hydraulic machine block, centrifugal regulator, low-pressure hydraulic system with booster and exhaust pipes.

The object of regulation in this problem is the frequency of alternating current, but taking the response speed of the electric part much more than the one of the constant speed drive, one can assume that the current frequency and generator rotor speed are connected by a constant coefficient. Therefore, let us write down the rotor motion equation:

$$J \cdot \frac{d\omega}{dt} = M_d - M_g - M_p - M_r, \text{ where}$$

J is the moment of inertia of the moments of inertia of the moving elements of the drive brought to the generator shaft; M_d is the driving torque; M_e is the torque on the generator rotor generated by the electric field; M_p is the torque on the crown gear being generated by the auxiliary pumps; M_r is the moment of mechanical loss brought to the output shaft of the drive.

$$M_g = \frac{N \cdot \cos\varphi}{\eta_g \cdot \omega}, \text{ where}$$

N is the load in power grid; ω is the rotor speed; η_g is the efficiency factor of generator.

The differential gear is a planetary gear which input link (pinion carrier — n) is connected to the input shaft of the drive. Output link - crown gear (b) transmits rotation to the generator shaft, sun gear (a) rotation from the hydraulic machine block. Pinion mates (g) and (f) being engaged with each other are connected by internal engagement to the crown and sun gears respectively. Axes of pinion mates are fixed in the pinion carrier. Figure 1 illustrates the kinematic scheme of the differential gear.

The relationship between the torques on the crown and sun gears of the differential gear is as follows:

$$M_b = M_a \cdot |i_{ab}^H| - M_{loss} \cdot (-1)^\alpha, \text{ where}$$

i_{ab}^H is the gear ratio between the sun and crown gears when the pinion carrier is stopped; α is the coefficient characterizing the mode of operation of the generator drive; M_{loss} is the moment of mechanical loss in the differential gear.

Kinematic relation for the planetary gear:

$$i_{ab}^n = \frac{\omega_b - \omega_n}{\omega_a - \omega_n}, \text{ where}$$

$\omega_n, \omega_b, \omega_a$ are the rotation speeds of the pinion carrier, the crown, and the sun gears respectively

The hydraulic machine block consists of two axial-plunger hydraulic machines of variable specific supply (HM_1) and constant specific supply (HM_2) connected by a hydraulic flow through a common distribution spool with two cavities of high and low pressures. The HM_1 hydraulic machine receives rotation from the pinion carrier, and its inclined washer can turn from an angle of $+\gamma$ to $-\gamma$. The gear of the HM_2 hydraulic machine shaft is engaged to the sun gear of the differential gear.

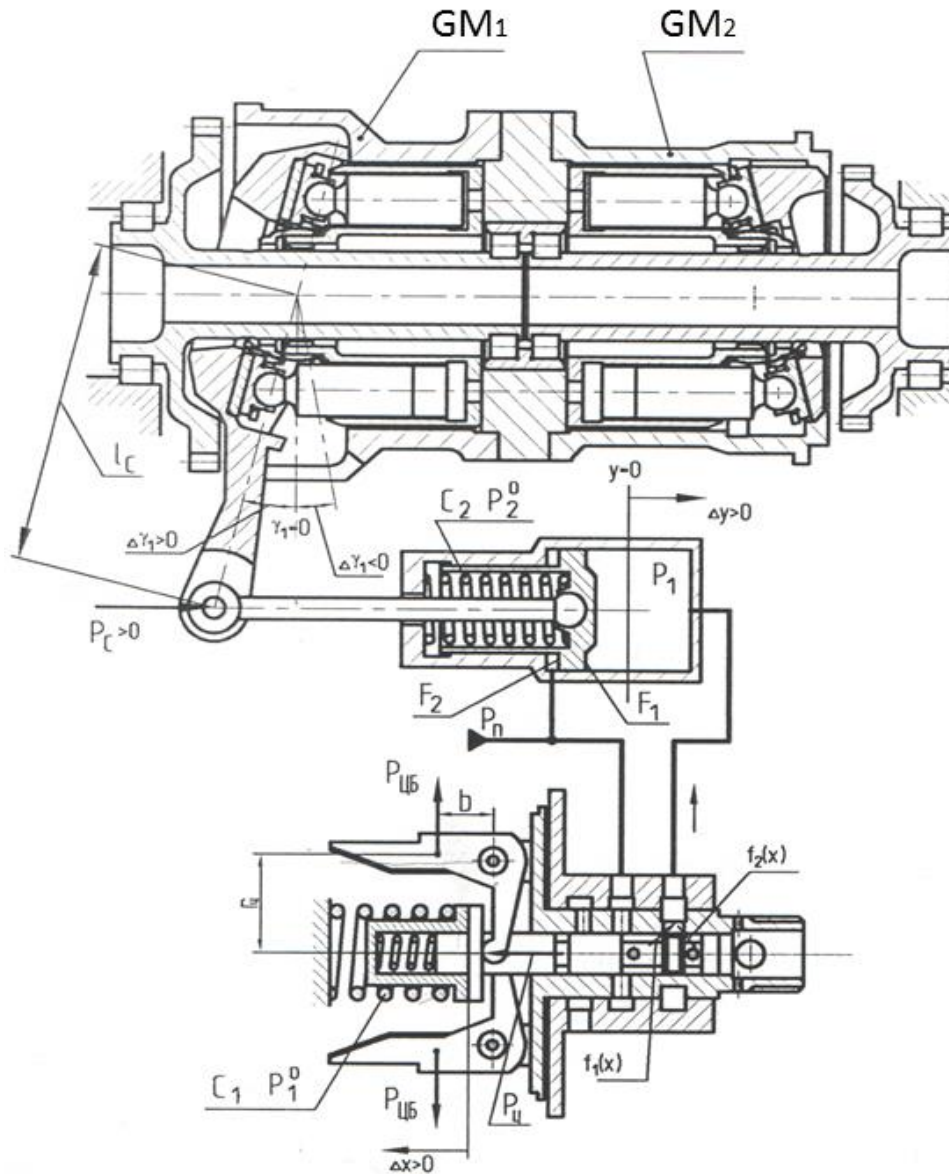


Fig.2.The diagram of the generator drive control system

The spool motion equation without taking into account the weight of spool and friction force:

$$P_1^0 + c_1 \cdot x = 2 \cdot m \cdot r_u \cdot \frac{b}{a} \cdot \omega_p^2, \text{ where}$$

P_1^0 is the spring force in position of tuning of a regulator to a rated frequency (400 Hz); c_1 is the spring stiffness; x is the spool travel; r_u is the distance between the centroid of the weights and spool axis; b is the distance between the centroid of the weights and rotation axis of the weights; a is the distance between the rotation axis of the weights to the centrifugal force application point; ω_p is the rotational frequency of the weights relative to the spool axis.

The servo piston motion equation:

$$P_2^0 + c_2 \cdot y + P_c = F_1 \cdot p_1 - F_2 \cdot p_n, \text{ where}$$

P_2^0 is the initial spring force; c_2 is the spring stiffness; F_1, F_2 is the area of the servo piston from the control pressure p_1 and booster pressure p_n ; P_c is the force acting on the servo piston from the inclined washer.

The equation of the relationship between the movements of the regulator spool and the servo piston:

$$F_1 \cdot \frac{dy}{dt} = \mu \cdot \sqrt{\frac{2}{\rho}} \cdot f_1(x) \cdot \sqrt{p_n - p_1} - \mu \cdot \sqrt{\frac{2}{\rho}} \cdot f_2(x) \cdot \sqrt{p_1 - p_k}, \text{ where}$$

$f_1(x), f_2(x)$ are the areas of clear openings of slots in the regulator sleeve on the pressure and drain edges when moving the spool; μ is the discharge ratio; ρ is the density of working fluid.

The relationship between the movement of the servo piston and the inclined washer with sufficient accuracy:

$$y = -\ell_c \cdot \gamma, \text{ where}$$

ℓ_c is the length of the lever of the inclined washer

The presented equations can be combined into one system, forming a mathematical model of GD:

$$\begin{cases} J \frac{d\omega}{dt} + \kappa_3 \omega = (\kappa_1 + 2\kappa_2) \kappa_2 \kappa_l \omega_n - \kappa_2 \kappa_l p_n - \frac{N \cos \varphi}{\eta_g \omega} - M_n - M_{loss} (-1)^\alpha \\ P_1^0 + c_1 \cdot x = 2 \cdot m \cdot r_u \cdot i_p^2 \cdot \frac{b}{a} \cdot \omega^2 \\ P_2^0 - c_2 \cdot \ell_c \cdot \gamma + P_c = F_2 \cdot p_1 - F_1 \cdot p_n \\ \frac{d\gamma_1}{dt} = \frac{-1}{\ell_c \cdot F_2} \cdot \left(\left(f_1(x) \cdot \sqrt{p_n - p_1} \right) - \sqrt{p_1 - p_k} \cdot \mu \cdot \sqrt{\frac{2}{\rho}} \right) \end{cases}, \text{ where}$$

$$\kappa_1 = \frac{q_1 \cdot \gamma_1}{2\pi \cdot \kappa_l} \cdot i_{21}; \quad \kappa_2 = \frac{q_2 \cdot \gamma_2}{2\pi \cdot \kappa_l} \cdot i_{34}; \quad \kappa_3 = \left(\frac{q_2 \cdot \gamma_2}{2\pi \kappa_l} \cdot i_{34} \right)^2 \cdot \kappa_l = \kappa_2^2 \cdot \kappa_l;$$

The analysis of the above model is conducted by its linear model, which is obtained by linearization of the system equations in the vicinity of a certain steady-state regime. By replacing variables with their increments, and derivatives with Laplace operators, and omitting intermediate transformations, we will obtain:

$$\begin{cases} (S + \kappa_{31}) \cdot \Delta\omega = \kappa_4 \cdot \Delta\omega_n - \kappa_N \cdot \Delta N - \kappa_\gamma \cdot \Delta\gamma_1 \\ \Delta x = \kappa_x \Delta\omega \\ S \Delta\gamma_1 = D \Delta x \end{cases}, \text{ where}$$

$$\kappa_{31} = \frac{\kappa_3}{J}; \quad \kappa_4 = (\kappa_1 + 2\kappa_2) \cdot \kappa_2 \cdot \kappa_l \cdot \frac{1}{J}; \quad \kappa_N = \frac{\cos \varphi}{\eta_r \omega_0 J};$$

$$\kappa_\gamma = \frac{q_1 \cdot i_{21}}{2 \cdot \pi} \cdot \frac{\kappa_2}{J} \cdot \omega_0; \quad \kappa_x = \frac{4 \cdot m \cdot i_p^2 \cdot \frac{b}{a} \cdot \omega_0 \cdot r_u^0}{c_1 - 2m \cdot i_p^2 \cdot \left(\frac{b}{a} \right)^2 \cdot \omega_0^2}; \quad D = \frac{\sigma}{\ell_c F_1};$$

$$\sigma = \mu \cdot \sqrt{\frac{2}{\rho}} \cdot \left(\frac{df_1^0(x)}{dx} \cdot \sqrt{p_n - p_1^0} - \frac{df_2^0(x)}{dx} \cdot \sqrt{p_1^0 - p_k^0} \right)$$

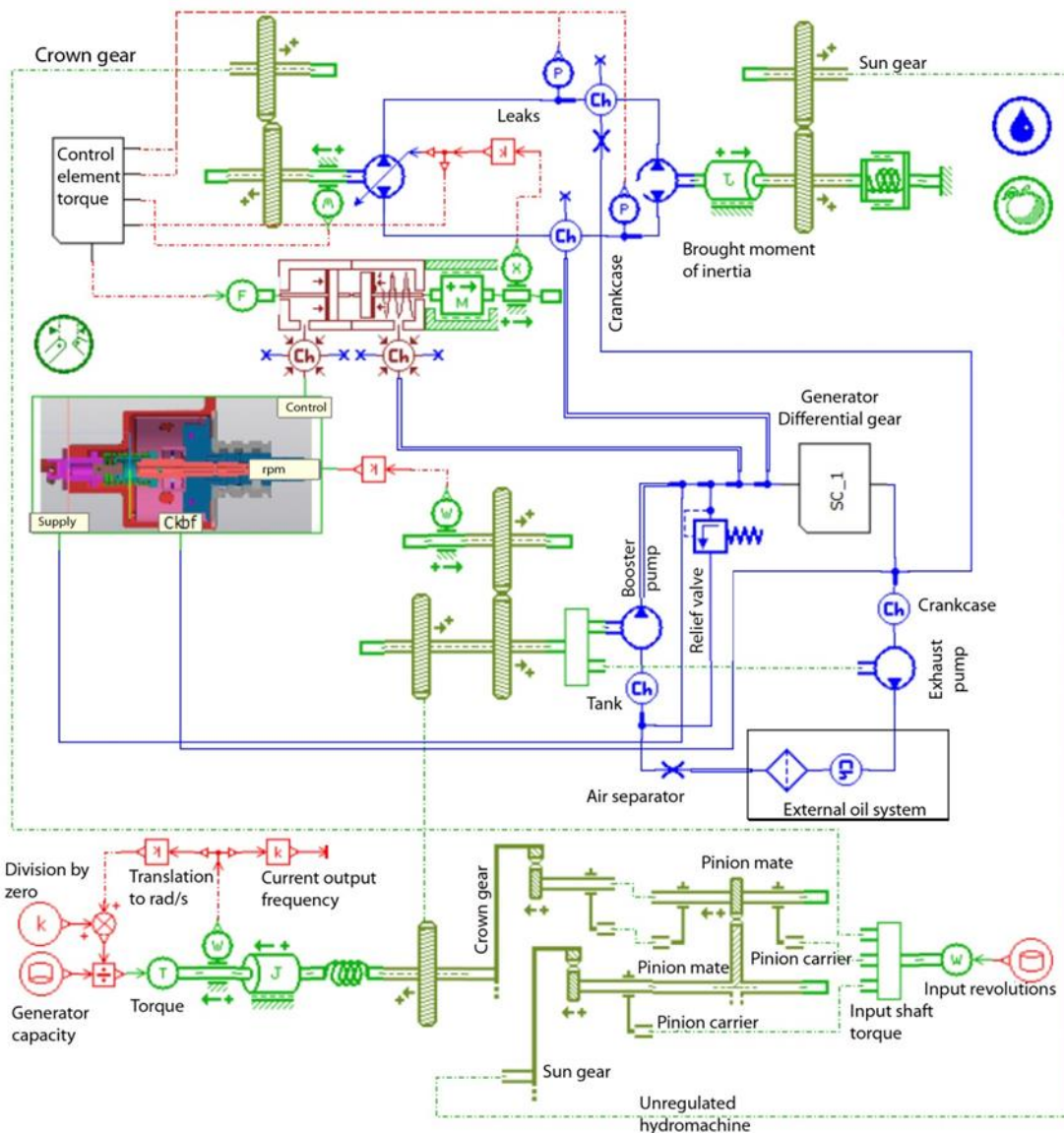


Fig.3.The generator drive model in AMESim

A single equation of this system, which relates the change in the rotation speed of the generator rotor with changes in speed of aircraft engine shaft and the load in the power grid, is an equation of the 2nd order:

$$(S^2 + \kappa_{31}S + \beta_c^2) \cdot \Delta\omega = \kappa_H \cdot S \cdot \Delta\omega_H - \kappa_N \cdot S \cdot \Delta N, \text{ where}$$

$\beta_c = \sqrt{\kappa_\gamma \cdot \kappa_X \cdot D}$ is the frequency of undamped natural oscillations.

The attenuation coefficient is determined by the equality:

$$\xi = \frac{\kappa_{31}}{2\beta_c}$$

In the expression of interest, the attenuation coefficient ξ is always greater than zero. Therefore, according to the Nyquist stability criterion, analytical model of GD is stable under any parameters of the unit.

The oscillability characterized by the attenuation coefficient largely depends on the magnitude of leaks from the power circuit of the hydraulic machines, i.e. the coefficient κ_{ym} . It is possible to obtain the following dependence:

$$\xi = f\left(\frac{1}{\sqrt{\kappa_l}}\right)$$

Since the friction pairs in the hydraulic machine wear out during operation, the leakage coefficient κ_l will increase over time, and at the same time the oscillability of the system will increase.

When generating a system model in the AMESim environment, numerous libraries of pre-tested components from various physical domains can be used. Thus, the GD model represents the blocks of gearing, hydrolines, inertial components, etc. connected to each other in a similar way to a real configuration of the unit. In contrast to the analytical GD model, in this case, the forces of dry and viscous friction, weights of the spool and servo piston, compressibility of liquid, and nonlinearity of the system in the form of the restriction of the rotation angle of the inclined washer, etc. are taken in account. Figure 3 illustrates the final model.

Results

To verify the models obtained, test data of the existing unit with rated power of 120 kW for a heavy cargo aircraft were applied. Figures 4 and 5 illustrate the responses of the AC frequency to the changes in the load in the test bench power grid and the input shaft rotation velocity. For the analytical model, the absence of a static error is true, while the value of the initial frequency jump and the nature of the transition process when the load changes in the power grid is close to the experimental data.

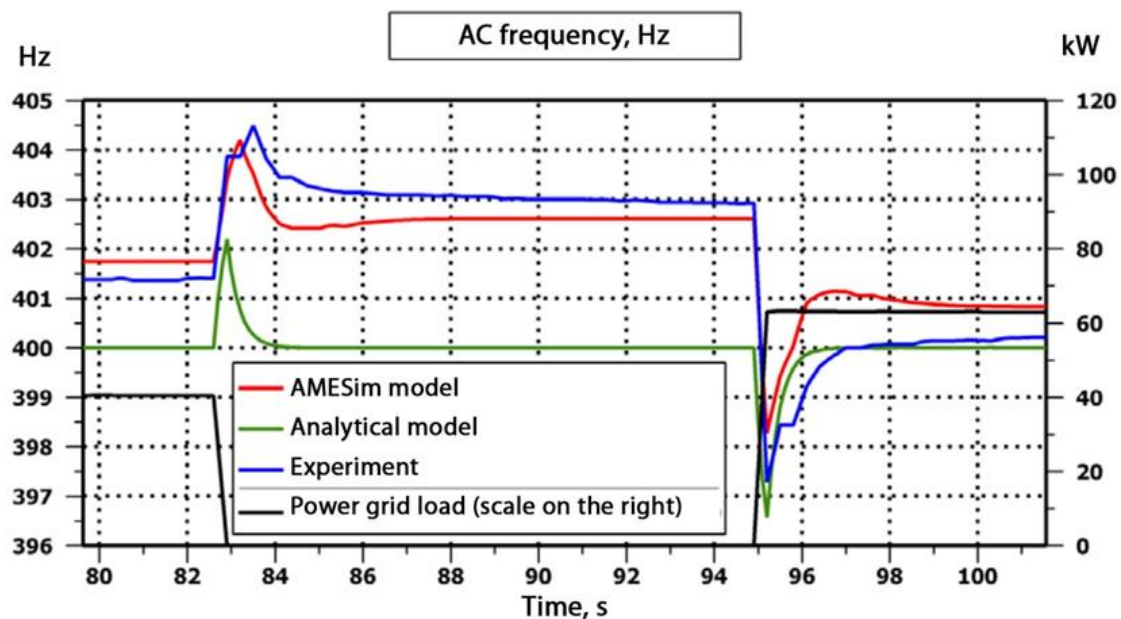


Fig.4. The response of AC frequency to a change of the load in power grid

The model prepared in AMESim has good convergence with the test data for both impacts. The value of the static error strongly depends on the size of gaps appeared during manufacture, level of filling, quality of execution of a particular unit, thus it is inexpedient to perform a comparison on steady-state modes.

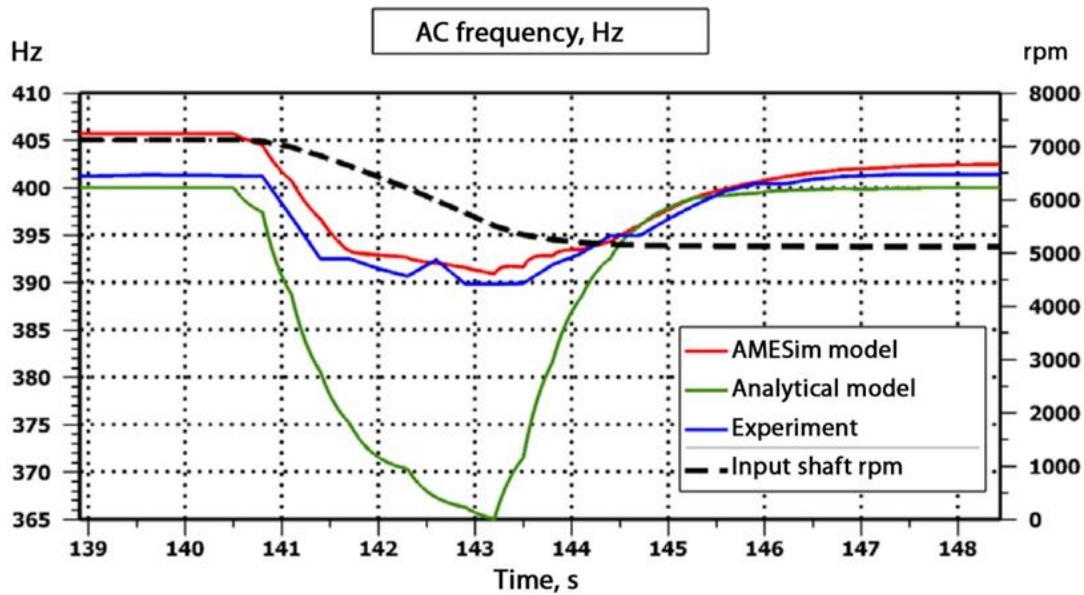


Fig. 5. The AC frequency response to a change in aircraft engine rpm

Conclusion

The analysis of the linear mathematical model has shown unconditional stability of the unit that is confirmed by the long-term experience of operation of the generator drives. The second conclusion is that the oscillability of the transient processes depends on the leakage coefficient and increases throughout the service life. However, cases of frequency mismatch due to severe wear and tear are extremely rare.

Using a model that takes into account the forces of dry and viscous friction, weight of the spool and servo piston, liquid compressibility, as well as the nonlinearity of the system allows to obtain results close to experimental data. Thus, the resulting model can be used as a tool for observing variables that are not available for direct measurement and used to synthesize the parameters of the regulator in order to obtain optimal transients.

Add in elements to the model that take into account thermal processes, as well as application of the CFD approach to calculate the internal flow of the working fluid is the next stage of the research.

References

- [1] S. Guo, J. Chen, Y. Lu, Y. Wang, H. Dong. Hydraulic piston pump in civil aircraft: Current status, future directions and critical technologies, Chinese Journal of Aeronautics, 2019, <https://doi.org/10.1016/j.cja.2019.01.013>.
- [2] I Kolodin and M Ryabinin 2019 IOP Conf. Ser.: Mater. Sci. Eng. 589 012018
- [3] Semenov, S., Kulakov, D. Mathematical modeling of the mechanisms of volumetric hydraulic machines (2019) IOP Conference Series: Materials Science and Engineering, 492 (1), article № 012042, .
- [4] Semenov, S.E. Mathematical modeling of the electro-hydraulic actuation systems of themachines with tree-like kinematic structure (2015) Proceedings of 2015 International Conference on Fluid Power and Mechatronics, FPM 2015, article № 7337184, pp. 583–592.
- [5] D Kulakov and B Kulakov 2019 IOP Conf. Ser. Mater. Sci. Eng. 492 012029
- [6] N Sosnovsky and D Ganieva 2019 IOP Conf. Ser.: Mater. Sci. Eng. 589 012016
- [7] A. Eid, H. El-Kishky, M. Abdel-Salam, T. El-Mohandes. Power Quality Investigations of VSCF Aircraft Electric Power Systems. 42nd South Eastern Symposium on System Theory, USA, March 7–9, 2010.

- [8] M. Mikhaylov, S. Stazhkov, V. Cvetkov. The Method of Disturbances Analysis on the Hydromechanical Constant Speed Drive. *Procedia Engineering*. 69.2014, 199–202. <https://doi.org/10.1016/j.proeng.2014.02.221>.
- [9] T. Jing , Y. Chengyu ,Y. Yaowen, S.Xudong. Simulation and Fault Detection for Aircraft IDG System. *Procedia Engineering*. 15. 2533–2537. (2011) <https://doi.org/10.1016/j.proeng.2011.08.476>.
- [10] Babaev, O.M.; Ignatov, L.N.; Kistochkin, E.S. &Cvetkov, V.A. (2000). Hydromechanical power transmissions, Mechanical engineering, St.-Petersburg, Russia.
- [11] Fornarelli F., LippolisA., OrestaP., PosaA., A computational model of axial piston swashplate pumps, *Energy Procedia*, Vol. 126, 2017, pp.1147–1154.
- [12] Junjun Z., Lingling J. Optimal Design of Hydraulic Position Servo-system Based on AMESim and Genetic Algrhythm. *Machine Tool and Hydraulic*, 2008, p.86–89.
- [13] Yongling F., XiaoyeQ. *AMESim System Modeling and Simulation*, BeiJing:Bei Jing University of Aeronautics Press, 2005.
- [14] Kalykin R., Perfil'evA., DruzhkovD., Elimination Of Erosion Phenomena Of A Cylinder Block Of Aircraft Axial Piston Hydraulic Machine, «*Nasosy. Turbina. Sistemy*» №4(29), 2018
- [15] Alessandro C., Massimo R., Comparison of 0D and 3D Hydraulic Models for Axial Piston Pumps, *Energy Procedia*, Volume 148, 2018, Pages 114–121, <https://doi.org/10.1016/j.egypro.2018.08.038>.